ELSEVIER

Journal of Materials Processing Technology 135 (2003) 30–43

Journal of Materials Processing Technology

www.elsevier.com/locate/jmatprotec

Constitutive models of steel under continuous casting conditions

Víctor D. Fachinotti*, Alberto Cardona

Centro Internacional de Métodos Computacionales en Ingeniería, INTEC, Universidad Nacional del Litoral/Conicet, Güemes 3450, Santa Fe 3000, Argentina

Received 26 November 2001; received in revised form 29 August 2002; accepted 24 September 2002

Abstract

We review in this paper a series of constitutive equations that describe the behavior of steels at elevated temperatures, laying emphasis upon continuous casting processes. The different laws are situated in an appropriate thermodynamic context, enabling the straightforward multiaxial generalization of uniaxial relationships proposed on a pure experimental basis. Plastic and viscoplastic standard materials are mainly considered, including models that split the instantaneous and creep components of the irreversible deformation. Unified models without a yield criterion are also treated. Predictions of different models for steels with the same carbon content are shown throughout the work.

Keywords: Materials; Steel constitutive models; Continuous casting; High temperature properties

1. Introduction

One of the major challenges of an accurate thermomechanical analysis of continuous casting processes is to obtain an adequate description of the complex relationships between stress, strain and time at elevated temperatures.

The simplest models take into account only the thermal deformation in the study of strand shrinkage and mold distortion, neglecting the mutual and external restrictions on the displacement field (and hence, on the total strain field).

Thermoelastic models satisfy these restrictions on total strain by considering a reversible (elastic) deformation, which is completely defined by the local current stress and temperature state. However, metals exhibit elastic response just within a region of the stress space. This so-called elastic region diminishes continuously as temperature increases, and disappears at the melting point. Therefore, modeling the high-temperature behavior of metals as elastic is but a rough approximation.

An improved model is achieved by considering an irreversible or inelastic strain, which is not only a function of the local current stress and temperature, but also of the history of stress (or strain) and temperature recorded at the considered point during the whole process.

Plasticity theory assumes that deformation is independent of the velocity at which deformation takes place. Plastic behavior is commonly observed in most metals at room temperature, that is, below one third of the absolute melting temperature. It is widely accepted that copper alloys that conform the mold may be modeled as plastic materials.

At elevated temperatures, materials become highly rate-sensitive. Viscoplastic models try to account for the strain rate dependence of irreversible deformation and constitute the most sophisticated laws to describe the response of cast metals.

The objective of this paper is to review a series of constitutive equations proposed for steel at high temperature by putting them in a thermodynamic framework. Thus, we develop the background for the multiaxial generalization of relationships defined from observation in uniaxial tests.

2. Thermodynamic framework

Following the *theory of local state* [1], we postulate that the thermodynamic state of a material at a given point and instant is completely defined by the so-called state variables at this point and instant. In this work we chose as state variables the total strain $\boldsymbol{\varepsilon}$, the absolute temperature T, the inelastic strain $\boldsymbol{\varepsilon}^{\mathrm{i}}$ and two strain-like hardening variables: a scalar, denoted r, that measures isotropic hardening, and a tensor, denoted $\boldsymbol{\alpha}$, that describes kinematic hardening. The isotropic hardening variable r is assumed to be equal to the

* Corresponding author.

0924-0136/02/$ – see front matter © 2002 Published by Elsevier Science B.V.
PII: S0924-0136(02)00955-X

Nomenclature

f	yield function
k	universal gas constant (=8.314 J mol^{-1} K^{-1})
t	time variable
$\dot{\lambda}$	consistency parameter
φ	dissipation potential
ψ	thermodynamic potential
State variables	
r	strain-like isotropic hardening variable (scalar)
R	stress-like isotropic hardening variable (scalar)
$\boldsymbol{s}$	Cauchy stress deviator
T	temperature
T_0	reference temperature
$\boldsymbol{X}$	stress-like kinematic hardening variable (tensor)
$\boldsymbol{\alpha}$	strain-like kinematic hardening variable (tensor)
$\boldsymbol{\varepsilon}$	total strain tensor
$\boldsymbol{\varepsilon}^{\mathrm{e}}$	elastic strain tensor
$\boldsymbol{\varepsilon}^{\mathrm{i}}$	inelastic strain tensor
θ	temperature variation (=$T - T_0$)
$\boldsymbol{\sigma}$	Cauchy stress tensor
σ_{eq}	von Mises equivalent stress
σ_{Y}	initial yield stress
Material properties	
A	coefficient in exponential and hyperbolic laws
c	carbon content
E	young modulus
E_{T}	elastoplastic Young's modulus
K	reference stress in Norton law
K_{p}	plastic resistance
M	hardening exponent
N	exponent in Norton law
Q	activation energy
α_{T}	thermal expansion coefficient
λ, μ	Lamé coefficients
κ	bulk modulus
ρ	density

equivalent inelastic strain accumulated in the time interval $[0, t]$, that is

$$r = \int_0^t \sqrt{\frac{2}{3}} \parallel \dot{\boldsymbol{\varepsilon}}^{\mathrm{i}}(\tau) \parallel \, \mathrm{d}\tau, \tag{1}$$

$\parallel \dot{\boldsymbol{\varepsilon}}^{\mathrm{i}} \parallel = \sqrt{\dot{\varepsilon}^{\mathrm{i}}_{ij}\dot{\varepsilon}^{\mathrm{i}}_{ij}}$ being the Euclidean norm of the second-order tensor $\dot{\boldsymbol{\varepsilon}}^{\mathrm{i}}$. A dotted variable denotes its time derivative.

When defining the relationships between these variables, we must keep in mind the thermodynamic restrictions imposed by the *Clausius–Duhem inequality*:

$$\boldsymbol{\sigma} \cdot \dot{\boldsymbol{\varepsilon}} - \rho(\dot{\psi} + s\dot{T}) - \frac{1}{T}\boldsymbol{q} \cdot \boldsymbol{g} \geq 0, \tag{2}$$

where $\boldsymbol{\sigma}$ is the stress tensor, s the entropy, ρ the density, ψ the specific Helmholtz free energy, $\boldsymbol{q}$ the heat flux vector, and $\boldsymbol{g} = \operatorname{grad} T$ the thermal gradient. Dots between two tensors denote the scalar product, defined either as the double contraction when applied to second-order tensors (e.g. $\boldsymbol{\sigma} \cdot \dot{\boldsymbol{\varepsilon}} = \sigma_{ij}\dot{\varepsilon}_{ij}$) or the simple contraction when applied to vectors (e.g. $\boldsymbol{q} \cdot \boldsymbol{g} = q_i g_i$).

Continuum thermodynamics [2] gives the basis to write thermodynamically admissible or stable constitutive equations. First, we postulate the existence of a *thermodynamic potential*, whose gradient defines the state laws. Our choice is Helmholtz energy, defined as a function of the state variables:

$$\psi(\boldsymbol{\varepsilon}, T, \boldsymbol{\varepsilon}^{\mathrm{i}}, r, \boldsymbol{\alpha}) = \psi^{\mathrm{e}}(\boldsymbol{\varepsilon} - \boldsymbol{\varepsilon}^{\mathrm{i}}, T) + \psi^{\mathrm{i}}(r, \boldsymbol{\alpha}, T). \tag{3}$$

This definition is consistent with the common assumption valid for small strains, namely the additive decomposition of the strain tensor:

$$\boldsymbol{\varepsilon} = \boldsymbol{\varepsilon}^{\mathrm{e}} + \boldsymbol{\varepsilon}^{\mathrm{i}}, \tag{4}$$

where $\boldsymbol{\varepsilon}^{\mathrm{e}}$ is the elastic (reversible) strain, including thermal expansion. Notice that the small strains assumption is widely accepted in the simulation of continuous casting processes, where total strains are usually below 2% [3]. Further, by virtue of Eq. (4), the elastic strain may take the place of the inelastic one as internal state variable.

From definition (3), the state laws take the form:

$$\boldsymbol{\sigma} = \rho \frac{\partial \psi}{\partial \boldsymbol{\varepsilon}^{\mathrm{e}}}, \tag{5}$$

$$s = -\frac{\partial \psi}{\partial T}, \tag{6}$$

$$R = \rho \frac{\partial \psi}{\partial r}, \tag{7}$$

$$\boldsymbol{X} = \rho \frac{\partial \psi}{\partial \boldsymbol{X}}, \tag{8}$$

with R and $\boldsymbol{X}$ denoting the thermodynamic forces associated to the internal variables r and $\boldsymbol{\alpha}$, respectively. Notice that the specification of ψ as a scalar function that is concave with respect to T and convex with respect to the other variables guarantees a priori the fulfillment of the Clausius–Duhem inequality.

2.1. Thermoelastic materials

For *linear elastic isotropic materials*, the thermodynamic potential takes the form

$$\psi \equiv \psi^{\mathrm{e}} = \frac{\lambda[\operatorname{Tr}(\boldsymbol{\varepsilon})]^2 + 2\mu \operatorname{Tr}(\boldsymbol{\varepsilon}^2) - 6\kappa\alpha_{\mathrm{T}}\theta \operatorname{Tr}(\boldsymbol{\varepsilon})}{2\rho} - \frac{C_\varepsilon}{2T_0}\theta^2, \tag{9}$$

so that

$$\boldsymbol{\sigma} = \lambda \operatorname{Tr}(\boldsymbol{\varepsilon}^{\mathrm{e}})\boldsymbol{I} + 2\mu\boldsymbol{\varepsilon}^{\mathrm{e}} - 3\kappa\alpha_{\mathrm{T}}\theta\boldsymbol{I}, \tag{10}$$

where λ and μ are the Lamé constants, $\kappa = (3\lambda + 2\mu)/3$ the bulk modulus, T_0 a reference temperature, $\theta = T - T_0$, C_ε

the specific heat at constant strain, α_T the thermal expansion coefficient, and $\boldsymbol{I}$ is the second-order identity tensor.

Eq. (9) implies small temperature variations ($\theta/T_0 \ll 1$) and hence its validity for continuous casting applications is questionable, specially for low carbon steels that suffer important volume changes during the δ–γ transformation. Thus, the thermal expansion $\alpha_T\theta$ is usually replaced by the linear expansion function [4]

$$\mathrm{TLE}(T, T_0) = \int_{T_0}^{T} \alpha_T(\vartheta)\,\mathrm{d}\vartheta, \tag{11}$$

that produces the former equation (10) for constant α_T.

The choice of purely thermoelastic models to characterize metal behavior at high temperatures leads to a simplified analysis. However, the thermoelastic solution can be used as an starting point for the iterative solution of the non-linear equations governing inelastic deformation processes, as done by Kelly et al. [5].

A thermoelastic model was also used by Ridolfi et al. [6] when studying the shrinkage of a continuously cast steel round billet to optimize mold taper. They determined the strand deformation by means of a purely thermal analysis with an empirical argument: they assumed the surface thermal strain matched the total strain averaged through the entire solidified shell thickness.

2.2. Elastic domain

It is often assumed that a material behaves elastically only within a limited region in the stress domain. This so-called elastic region is bounded by the yield surface, which is defined here using the von Mises criterion:

$$f(\boldsymbol{\sigma}, R, \boldsymbol{X}) = \sqrt{\tfrac{3}{2}}\,\| \boldsymbol{s} - \boldsymbol{X} \| - (\sigma_Y + R) = 0, \tag{12}$$

where $\boldsymbol{s} = \mathrm{dev}(\boldsymbol{\sigma})$ is the deviatoric part of the stress tensor, σ_Y is the initial yield stress under tensile test conditions, R controls the size of the elastic domain and $\boldsymbol{X}$ defines its center in the stress-deviator space.

2.3. Characterization of dissipative processes

When deformation is no longer elastic, we need complementary constitutive equations that describe the evolution of the internal variables $\boldsymbol{\varepsilon}^i$, r and $\boldsymbol{\alpha}$. To this end, we postulate the existence of a new potential, the so-called *dissipation potential*

$$\varphi = \varphi(\boldsymbol{\sigma}, R, \boldsymbol{X}, \boldsymbol{g}), \tag{13}$$

from which the evolution laws are derived by means of the *normality rule*:

$$\dot{\boldsymbol{\varepsilon}}^i = \frac{\partial \varphi}{\partial \boldsymbol{\sigma}}, \tag{14}$$

$$-\dot{r} = \frac{\partial \varphi}{\partial R}, \tag{15}$$

$$-\dot{\boldsymbol{\alpha}} = \frac{\partial \varphi}{\partial \boldsymbol{X}}, \tag{16}$$

$$-\frac{\boldsymbol{q}}{T} = \frac{\partial \varphi}{\partial \boldsymbol{g}}. \tag{17}$$

By requiring $\varphi(\boldsymbol{\sigma}, R, \boldsymbol{X}, \boldsymbol{g})$ to be a convex function of $\boldsymbol{\sigma}$, r, $\boldsymbol{\alpha}$, and $\boldsymbol{g}$, so that $\varphi = 0$ at the origin, the normality rule forces the Clausius–Duhem inequality to hold automatically. Therefore, the normality rule is a sufficient (but not necessary) condition for thermodynamic stability.

In the following analysis, the heat flow law, Eq. (17), will not be taken into account. Furthermore, temperature T will not be considered as a state variable but as a parameter upon which the material properties depend in the formulation of constitutive equations.

Materials whose evolution is completely defined by the normality rule, i.e. Eqs. (14)–(16), are called *generalized standard materials*. If only its flow rule is verified, Eq. (14), the material is simply called *standard*. We should mention that when describing the standard material formulation, we closely follow the work by Lemaître and Chaboche [1].

3. Plasticity

For rate-independent behavior, the dissipation potential φ is non-differentiable, but we can think of φ as the indicator function of the convex set defined by $f = 0$ (the closure of the elastic domain), and then rewrite the evolution laws (14)–(16), as follows:

$$\dot{\boldsymbol{\varepsilon}}^i = \dot{\lambda}\frac{\partial F}{\partial \boldsymbol{\sigma}}, \tag{18}$$

$$-\dot{r} = \dot{\lambda}\frac{\partial F}{\partial R}, \tag{19}$$

$$-\dot{\boldsymbol{\alpha}} = \dot{\lambda}\frac{\partial F}{\partial \boldsymbol{X}}, \tag{20}$$

where F is the *flow potential*, and $\dot{\lambda}$ is the consistency parameter, satisfying the *Kuhn–Tucker conditions*:

$$\dot{\lambda} \geq 0, \quad f \leq 0, \quad \dot{\lambda} f = 0, \tag{21}$$

and the *consistency condition*

$$\dot{\lambda}\dot{f} = 0. \tag{22}$$

From now on, we restrict ourselves to the *associative theory of plasticity* adopting the yield function f as flow potential.

3.1. Plasticity with isotropic hardening

This hypothesis implies $\boldsymbol{X} = \boldsymbol{0}$. As aforementioned, the equivalent accumulated plastic strain plays the role of hardening variable. Let us assume that the material obeys the von Mises yield criterion, while the hardening curve $R(r)$ is defined by the *Ramberg–Osgood law* [1]

$$R(r) = K_p r^{1/M}, \tag{23}$$

where K_p and M are thermodependent material properties called plastic resistance and hardening exponent, respectively. After using the consistency condition, Eq. (22), the following flow law is obtained:

$$\dot{\boldsymbol{\varepsilon}}^{i} = \frac{3}{2}\frac{M}{K_p}\left\langle \frac{\sigma_{eq} - \sigma_Y}{K_p} \right\rangle^{M-1} \langle \dot{\sigma}_{eq} \rangle \frac{\boldsymbol{s}}{\sigma_{eq}}, \tag{24}$$

where $\sigma_{eq} = \sqrt{3/2} \parallel \boldsymbol{s} \parallel$ is the equivalent von Mises stress, and $\langle x \rangle = (1/2)(x + |x|)$ is the so-called ramp function ($\langle \cdot \rangle$ are also known as Macauley brackets) [7].

We do not need to invoke the evolution equation (19) for the hardening variable r; in fact, since r has been assimilated to the equivalent inelastic strain defined by Eq. (1), its evolution equation

$$\dot{r} = \sqrt{\frac{2}{3}} \parallel \dot{\boldsymbol{\varepsilon}}^{i} \parallel = \frac{M}{K_p}\left\langle \frac{\sigma_{eq} - \sigma_Y}{K_p} \right\rangle^{M-1} \langle \dot{\sigma}_{eq} \rangle, \tag{25}$$

can be straightforwardly derived from the flow rule (24).

Applications: Whenever models of this kind are used, a single characteristic value of strain rate is adopted for the analysis, which may range from 10^{-5} to $10^{-2}\ s^{-1}$ in continuous casting processes.

Uehara et al. [8] applied an elastoplastic model with nonlinear isotropic hardening ($M \neq 1$ in the Ramberg–Osgood law) for the study of bulging and unbending in steel slabs produced by a low-head bow type continuous casting machine. For low carbon steels, they assumed that the initial yield stress σ_Y depends on temperature, while the plastic resistance K_p is constant. On the other hand, the strain exponent $1/M$ was assumed to depend on the Zener–Hollomon parameter:

$$Z = \dot{\varepsilon} \exp\left[\frac{Q}{kT}\right],$$

Q being the material activation energy and k the universal gas constant. Z was determined from estimates of the strain rate $\dot{\varepsilon}$ and temperature. Unfortunately, numerical data for this model were not published, so that we could not take it into account for comparison purposes.

The rest of the plastic laws we found in the literature of continuous casting processes assumed linear isotropic hardening ($M = 1$) and followed the work of Kelly et al. [5]. In most cases, the analysis was devoted to the simulation of the early stages of steel round billet continuous casting processes. The characteristic strain rate was usually estimated in the order of $10^{-4}\ s^{-1}$. Since the consistency condition is amenable to closed-form solution, this formulation is very convenient from the computational point of view [7].

In the widely quoted work of Kelly et al., the proposed model was addressed to describe the behavior of several carbon steels (0.1, 0.4, and 0.7 wt.% C) under the above mentioned conditions. The initial yield stress σ_Y, the elastoplastic tangent modulus E_T, and the Young modulus E, were calculated using Wray's tensile test data [9] at a constant strain rate of $4 \times 10^{-4}\ s^{-1}$. The plastic resistance K_p, which is equal to the hardening modulus $R' = dR/dr$ in the linear hardening case, may then be computed as $K_p = EE_T/(E - E_T)$.

Dvorkin and Canga [10], Huespe et al. [11], and Cardona et al. [12] applied Kelly's model to represent a 0.4 wt.% C steel (in the latter work, a 0.1 wt.% C steel was also modeled). The same model has been applied by Rugonyi et al. [13], who fitted Wray's data at a strain rate of $1.5 \times 10^{-4}\ s^{-1}$ using a linear isotropic hardening model to describe the behavior of a (0.28 wt.% C, 1.30 wt.% Mn) steel. Also, Huespe et al. [14] represented a plain carbon steel (0.4 wt.% C) as a plastic material with linear isotropic hardening, and in this case material properties were

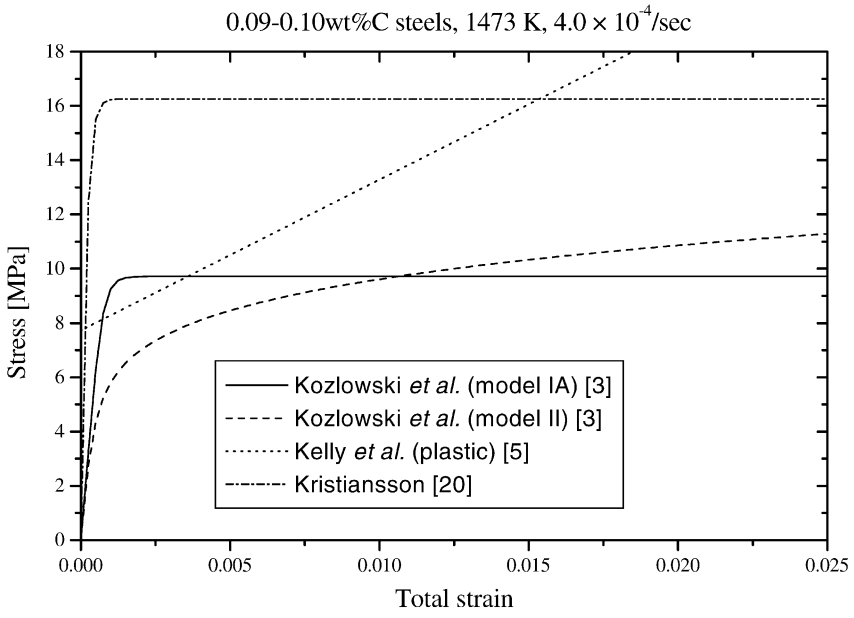

Fig. 1. Tensile curves for low carbon steels.

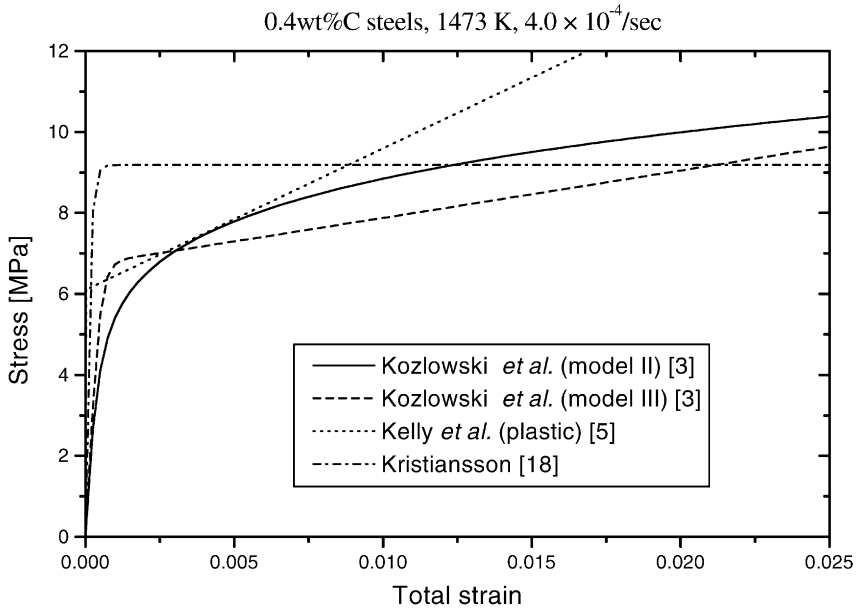

Fig. 2. Tensile curves for medium carbon steels.

adjusted to best-fit Kozlowski et al.'s viscoplastic model III [3] (see Table 1) under tensile test conditions at 1.4×10^{-4} s^{-1}.

Fig. 1 plots the tensile curve for 0.09–0.1 wt.% C steels at a temperature of 1473 K, as predicted by Kelly's plastic (P) model, compared to those produced by several viscoplastic (VP) models at the characteristic strain rate of 4×10^{-4} s^{-1} assumed by Kelly et al. Fig. 2 shows curves by models of the same authors, but for 0.4 wt.% C steels.

Fig. 3 compares results of the Huespe et al.'s elastic/plastic model, which was proposed for a strain rate of 1.4×10^{-4} s^{-1}, with those given by viscoplastic models of steel.

In Fig. 4, Kelly et al.'s prediction of the behavior of 0.7 wt.% C (eutectic) steels at 1373 K is compared to Wray's experimental data and to a viscoplastic solution for a strain rate of 4.0×10^{-4} s^{-1}.

4. Viscoplasticity

4.1. Perfect viscoplasticity

This model assumes that inelastic flow occurs at constant rate, which is typical of the secondary creep phase. In such

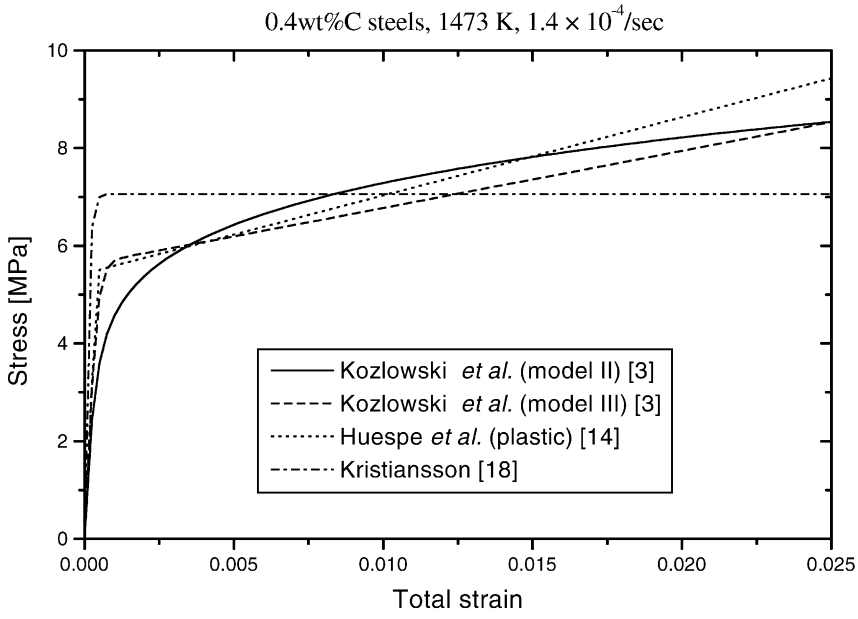

Fig. 3. Tensile curves for medium carbon steels.

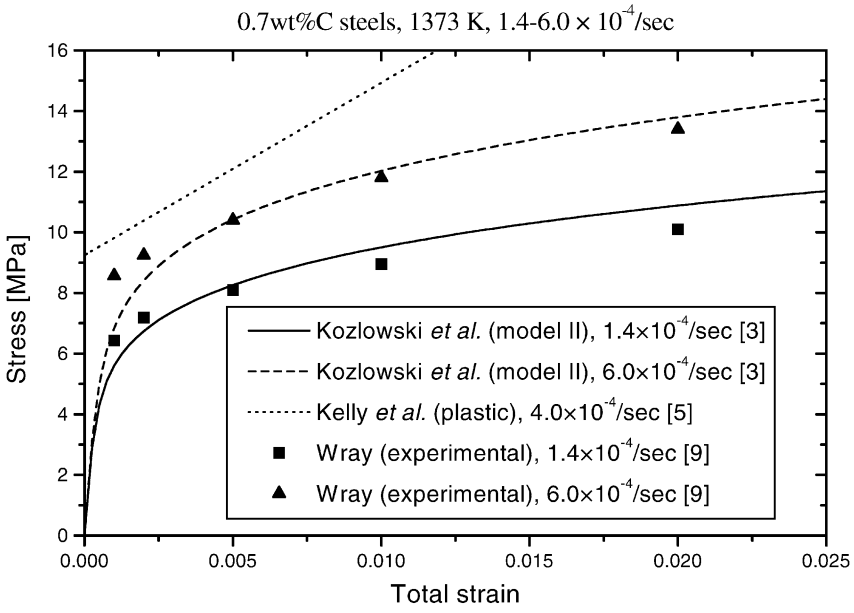

Fig. 4. Tensile curves for eutectic steels.

case, hardening variables are not necessary. *Odqvist's law* is written:

$$\dot{\boldsymbol{\varepsilon}}^{\mathrm{i}} = \frac{3}{2}\left(\frac{\sigma_{\mathrm{eq}}}{K}\right)^{N}\frac{\boldsymbol{s}}{\sigma_{\mathrm{eq}}}, \tag{26}$$

and can be derived from the potential

$$\varphi = \frac{K}{N+1}\left(\frac{\sigma_{\mathrm{eq}}}{K}\right)^{N+1}. \tag{27}$$

This law describes a perfectly viscoplastic material; K and N are material properties that may depend on temperature. Odqvist's law is the multiaxial generalization of the well-known *Norton law*:

$$\dot{\varepsilon}^{\mathrm{i}} = \left(\frac{\sigma_{\mathrm{eq}}}{K}\right)^{N}. \tag{28}$$

Here, tensors are represented in bold, while their counterpart in italics represent the same quantity in a uniaxial condition; e.g. $\boldsymbol{\varepsilon}^{\mathrm{i}}$ is the inelastic strain and ε^{i} is the deformation measured in a uniaxial test. Under monotonic loads, the absolute value of ε^{i} equals the equivalent inelastic strain r, justifying the inclusion of the factor $\sqrt{2/3}$ in definition (1). Furthermore, the uniaxial stress σ equals σ_{eq} for arbitrary uniaxial loading. Whenever we refer to uniaxial constitutive laws, their multiaxial extension implies the assimilation of σ to σ_{eq} and ε^{i} to r, which is only valid under monotonic loading.

Applications: Sakui and Sakai [15] modeled a low carbon steel (0.16 wt.% C, 0.31 wt.% Si, 0.52 wt.% Mn, 0.008 wt.% P, 0.006 wt.% S) within the austenitic range and a wide range of strain rates (1.43×10^{-1} to 2.73×10^{-5} s^{-1}) (conditions that apply in continuous casting processes) using the following secondary creep law:

$$\dot{\varepsilon} = C\exp\left(-\frac{Q}{kT}\right)\sigma^{N}, \tag{29}$$

where $C = 3.996\ \mathrm{MPa}^{-N}\ \mathrm{s}^{-1}$, $N = 5.4$, and $Q = 286.74$ kJ mol^{-1} are constant material properties. The latter equation becomes the Norton law either by the usual hypothesis of fully-developed flow ($\dot{\varepsilon} \approx \dot{\varepsilon}^{\mathrm{i}}$) or by neglecting elastic deformation, and making:

$$K = C^{-1/N}\exp\left(\frac{Q}{NkT}\right). \tag{30}$$

Eq. (29) exhibits a common feature of a wide class of viscoplastic models that define creep as a thermally activated phenomenon governed by the *Arrhenius law*:

$$\dot{\varepsilon}^{\mathrm{i}} \propto \exp\left(-\frac{Q}{kT}\right). \tag{31}$$

Remark. From now on, units of stress are MPa, the strain is given in m/m (non-dimensional), the strain rate in s^{-1}, the ratio Q/k and the temperature are given in K, and units of the coefficient C are such that the concerned equation is dimensionally correct.

Grill and Sorimachi [16] referred to Sakui and Sakai in the study of bulging of continuously cast steel slabs. They also applied a secondary creep law identical in form to Eq. (29) for a ferritic iron (Fe–3Si), where $C = 1566$, $Q/k = 24\,264$, and $N = 3.77$. They reported that the former model underestimates the slab bulging, while the latter exaggerates it, when compared to experimental measurements.

Dalin and Chenot [17] also employed a secondary creep law when studying bulging in continuous casting of steel slabs of a 18M5 steel (0.18 wt.% C, 1.37 wt.% Mn). Their model turns out to be the Odqvist's law under the assumption of fully-developed flow or negligible elastic strains. The

strain rate sensitivity $1/N$ is assumed constant (=0.141), while K is defined as

$$K = 0.389 \exp\left(\frac{7680}{T}\right)\bar{\varepsilon}_0^{0.182},$$

$\bar{\varepsilon}_0 \approx 0.003$ being an average strain dependent on the refinement of the finite element mesh used for computations.

Kristiansson [18] used the Odqvist's law for the analysis of the thermal stresses that arise during the early stages of solidification of steels, specifically for 0.09 and 0.40 wt.% C steels. A distinctive feature of Kristiansson's model, is that the material property $B = K^{-N}$ (usually called fluidity, or inverse viscosity) is defined as a piece-wise linear monotonically increasing function of temperature, instead of the exponential activation energy term defined by the Arrhenius law. Fig. 1 shows a comparison between this model and other models applied to 0.4 wt.% C steels.

Kozlowski et al.'s model IA [3] for steels at elevated temperatures (austenitic range) and low strain rates (10^{-3} to 10^{-6} s^{-1}), is very similar in form to Eq. (29), in which the inelastic strain $\dot{\varepsilon}^{i}$ takes the place of the total strain $\dot{\varepsilon}$. In this model, as well as in the other models by Kozlowski et al. to be introduced later, material property c takes into account the carbon content C and plays the role of a scaling factor to adjust the constitutive equations to a wide range of plain carbon steels (0.005–1.54 wt.% C). This feature allows us to apply Kozlowski et al.'s models as test cases for comparison purposes, as it can be seen in all plots in this work. Kozlowski et al.'s standard viscoplastic models are listed in Table 1.

El-Bealy [19] proposed a secondary creep law with $N = 3.313$ and $K = 7.27 \times 10^{-3}\ (T_{liq} - T)^{1.791}$, T_{liq} being the liquidus temperature, to represent the behavior of low alloy carbon steels (0.12, 0.136, and 0.143 wt.% C) from the beginning of the unbending of continuously cast slabs. Here, the power law $(T_{liq} - T)^{1.791}$ replaces the Arrhenius exponential law for the description of thermally activated creep flows. For the early stages of casting, El-Bealy chose a primary creep material law that will be described later when dealing with multiplicative viscosity-hardening models.

Fig. 5 shows the constant strain rate (1.4×10^{-4} s^{-1}) hardening curves for 0.12–0.15 wt.% C steels at 1573 K, including the laws of El-Bealy and Thomas et al. previously described.

Figs. 6 and 7 display tensile curves for low carbon steels (0.16–0.19 wt.% C content) at constant temperatures (1373 and 1473 K) and strain rate (1.4×10^{-4} s^{-1}). In these figures, the Norton-type models of Sakui and Sakai, Dalin and Chenot (with $\bar{\varepsilon}_0 = 0.003$) and Kozlowski et al. are compared.

4.1.1. Odqvist's law with elastic range

In this model, the existence of a (constant) elastic domain whose size is defined by the initial yield stress σ_Y is

Table 1
Kozlowski et al.'s standard viscoplastic models for steel [3]

Perfect viscoplasticity	
Model IA: *Norton law*	
Flow rule	$\dot{\varepsilon}^{i} = C\exp[-Q/(kT)]\sigma^N$
Material parameters	$Q/k = 49\,890$
	$N = 5.331 + 4.116 \times 10^{-3}T - 2.116 \times 10^{-6}T^2$
	$C = 24\,333 + 49\,973c + 48\,757c^2$
Model IB: *hyperbolic law*	
Flow rule	$\dot{\varepsilon}^{i} = C\exp[-Q/(kT)]\sinh(a_\sigma\sigma)$
Material parameters	$Q/k = 56\,423$
	$a_\sigma = 1.5403 + 5.913 \times 10^{-5}T - 5.538 \times 10^{-7}T^2$
	$C = 2.602 \times 10^{10} + 2.265 \times 10^{12}c - 1.332 \times 10^{12}c^2$
Model IC: *hyperbolic law*	
Flow rule	$\dot{\varepsilon}^{i} = C\exp[-Q/(kT)]\sinh^N(a_\sigma\sigma)$
Material parameters	$Q/k = 44\,809$
	$N = 0.200 + 3.966 \times 10^{-4}T$
	$a_\sigma = 1.068 + 1.702 \times 10^{-4}T - 2.808 \times 10^{-7}T^2$
	$C = 1.802 \times 10^{6} + 1.742 \times 10^{8}c - 6.503 \times 10^{7}c^2$
Viscoplasticity with hardening	
Model II: *multiplicative-viscosity hardening law*	
Flow rule	$\dot{\varepsilon}^{i} = \tilde{C}\exp[-\tilde{Q}/(kT)]\sigma^n t^m$
Material parameters	$\tilde{Q}/k = 17\,160$
	$n = 6.365 - 4.521 \times 10^{-3}T + 1.439 \times 10^{-6}T^2$
	$m = -1.362 + 5.761 \times 10^{-4}T + 1.982 \times 10^{-8}T^2$
	$\tilde{C} = 0.3091 + 0.2090c + 0.1773c^2$
Model III: *additive-viscosity hardening law*	
Flow rule	$\dot{\varepsilon}^{i} = C\exp[-Q/(kT)]\langle\sigma_{eq} - a_\varepsilon\varepsilon^{i^{n_\varepsilon}}\rangle^N$
Material parameters	$Q/k = 44\,650$
	$N = 8.132 - 1.540 \times 10^{-3}T$
	$a_\varepsilon = 130.5 - 5.128 \times 10^{-3}T$
	$n_\varepsilon = -0.6289 + 1.114 \times 10^{-3}T$
	$C = 46\,550 + 71\,400c + 12\,000c^2$

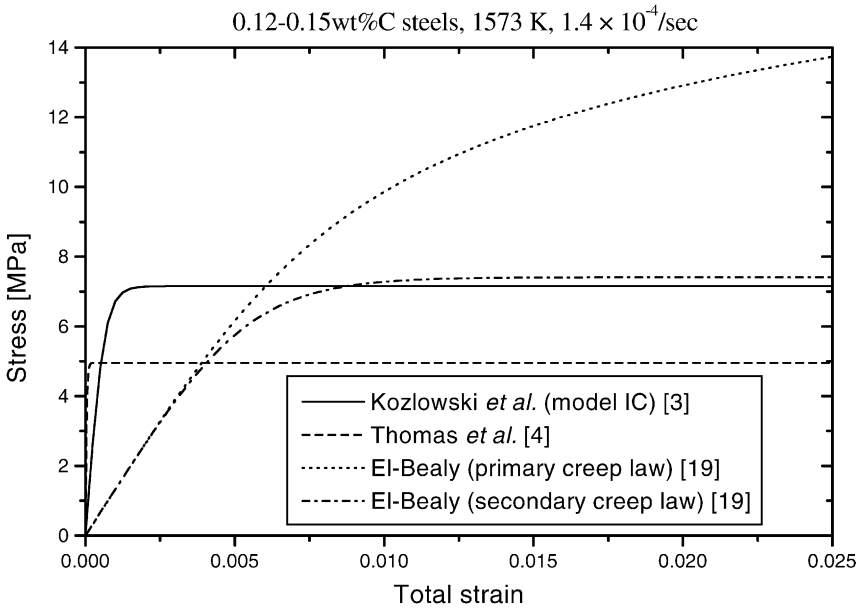

Fig. 5. Tensile curves for low carbon steels.

assumed. Odqvist's law can be extended to this case as follows:

$$\dot{\boldsymbol{\varepsilon}}^{\mathrm{i}} = \frac{3}{2}\left\langle \frac{\sigma_{\mathrm{eq}} - \sigma_{\mathrm{Y}}}{K} \right\rangle^{N} \frac{\boldsymbol{s}}{\sigma_{\mathrm{eq}}}. \tag{32}$$

This definition is consistent with a dissipation potential expressed as

$$\varphi = \frac{K}{N+1}\left\langle \frac{\sigma_{\mathrm{eq}} - \sigma_{\mathrm{Y}}}{K} \right\rangle^{N+1}. \tag{33}$$

Applications: Williams et al. [20], Lewis et al. [21], and Inoue [22], proposed a simplified form of Eq. (33), assuming $N = 1$, for the study of metal casting problems. Bellet et al. [23] also proposed an extended Odqvist's law for the thermomechanical analysis of metals during the cooling stage of casting processes, although their model is applied to aluminum casting.

4.1.2. Exponential and hyperbolic laws

In many cases, experimental evidence shows that the net-stress exponent N tends to increase for low values of stress.

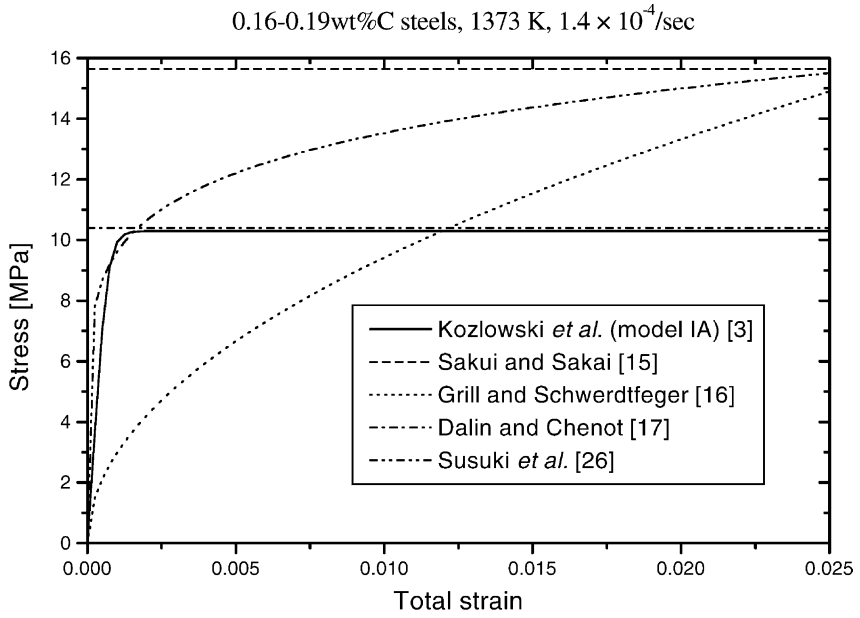

Fig. 6. Tensile curves for low carbon steels.

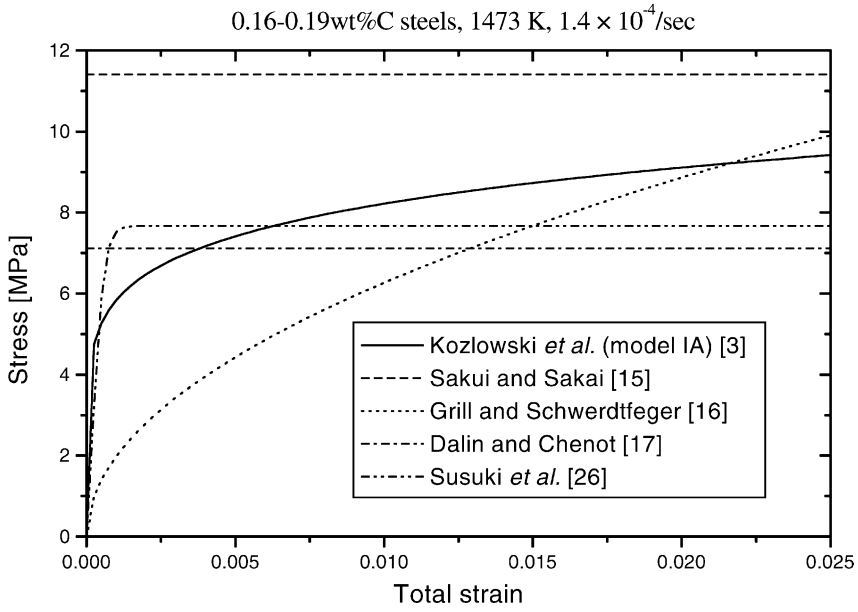

Fig. 7. Tensile curves for low carbon steels.

Odqvist's law, Eq. (26), may be modified to account for this phenomenon by writing the potential as

$$\varphi = \frac{\exp(A\sigma_{\text{eq}}^{N+1})}{A(N+1)K^N}, \tag{34}$$

where A is the material property. The following flow rule is then obtained:

$$\dot{\boldsymbol{\varepsilon}}^{\text{i}} = \frac{3}{2}\dot{r}\frac{\boldsymbol{s}}{\sigma_{\text{eq}}}, \tag{35}$$

$$r = \left(\frac{\sigma_{\text{eq}}}{K}\right)^N \exp(A\sigma_{\text{eq}}^{N+1}). \tag{36}$$

An alternative to the exponential law is the hyperbolic law

$$\dot{r} = A\left(\sinh\frac{\sigma_{\text{eq}}}{K}\right)^N. \tag{37}$$

Applications: Kozlowski et al.'s models IB and IC [3] can be thought of as uniaxial expressions of the hyperbolic law under monotonic loads:

$$\dot{\varepsilon}^{\text{i}} = C\exp\left(-\frac{Q}{kT}\right)[\sinh(a_\sigma\sigma)]^N, \tag{38}$$

where coefficients in Eq. (37) are

$$A = C\exp\left[-\frac{Q}{kT}\right], \qquad K = a_\sigma^{-1}.$$

Material properties for both models are listed in Table 1. Fig. 5 shows an application of model IC.

Other hyperbolic laws, with $N > 1$, were applied in the work of Thomas et al. [4] to simulate medium carbon steels (0.46 wt.% C) in the austenitic range,

$$\dot{r} = 9.07\times10^{10}\exp\left(-\frac{41\,938}{T}\right)[\sinh(0.035\sigma_{\text{eq}})]^{6.90}. \tag{39}$$

To simulate low carbon steels (0.15 wt.% C), the same work proposed

$$\dot{r} = A_0\exp\left(-\frac{39\,600}{T}\right)[\sinh(0.0741\sigma_{\text{eq}})]^{5.98}, \tag{40}$$

with

$$A_0 = \begin{cases} 4.2\times10^{12} & \text{for } T < Ar_1, \\ 4.2\times10^{9} & \text{for } T > Ar_3, \end{cases}$$

Ar_3 and Ar_1 are the start and finish temperatures of the austenite to ferrite/pearlite transformation during the cooling process. Therefore, Eq. (40) aims to simulate the accelerated creep in the softer ferrite phase of low carbon steels. Fig. 5 shows this law evaluated at $1.4\times10^{-4}\ \text{s}^{-1}$ and 1573 K.

Li and Ruan [24] developed a similar model for thermal stress analysis in continuous casting, assuming all material properties in Eq. (38) to be constant. Still, their model is not particularly addressed to steel but to aluminum casting.

4.2. Viscoplasticity with isotropic hardening

4.2.1. Additive viscosity-hardening law

So far, we considered a constant elastic range of size σ_{Y} in the potential (33) by defining an extended Odqvist's law. Now, we define a potential that accounts for a variable elastic range, whose size is measured by $\sigma_{\text{Y}} + R$, where R gives the value of hardening:

$$\varphi = \frac{K}{N+1}\left\langle\frac{\sigma_{\text{eq}} - R - \sigma_{\text{Y}}}{K}\right\rangle^{N+1}. \tag{41}$$

Normality rules produce then the following flow rule:

$$\dot{\boldsymbol{\varepsilon}}^{\text{i}} = \frac{3}{2}\dot{r}\frac{\boldsymbol{s}}{\sigma_{\text{eq}}}, \tag{42}$$

$$\dot{r} = \left\langle \frac{\sigma_{eq} - R - \sigma_Y}{K} \right\rangle^N. \tag{43}$$

Applications: The additive law has been used by Huespe et al. [25] to model high temperature steel behavior, in the form

$$\dot{r} = C \exp\left(-\frac{Q}{kT}\right) \langle \sigma_{eq} - a_\varepsilon r^{n_\varepsilon} \rangle^N, \tag{44}$$

where the Ramberg–Osgood hardening law, Eq. (23), is implied. The initial elastic limit is assumed to be negligible ($\sigma_Y = 0$) and K is defined by Eq. (30). Material parameters in Eq. (44) were taken from Kozlowski et al.'s model III [3], which is detailed in Table 1. In fact, Huespe et al.'s model is a modification of Kozlowski et al.'s model III, to which it is reduced in the case of monotonic loading. Reasons for this modification will be discussed later in the context of kinematic hardening models.

4.2.2. Multiplicative viscosity-hardening law

We postulate a dissipation potential as:

$$\varphi = \varphi^*(\sigma_{eq} - R - \sigma_Y + h'(r))\xi(r) \tag{45}$$

with the thermodynamic potential:

$$\psi = \psi^e + \frac{1}{\rho} h(r), \tag{46}$$

and $h' = \mathrm{d}h/\mathrm{d}r$. Here, $h(r)/\rho = \psi^i$ is the *inelastic free energy* (see Eq. (3)).

Usually, φ^* and ξ are power functions,

$$\varphi = \frac{K}{N+1} \left\langle \frac{\sigma_{eq} - R - \sigma_Y + h'(r)}{K} \right\rangle^{N+1} r^\gamma, \tag{47}$$

from which the following flow rule is derived:

$$\dot{r} = -\frac{\partial \varphi}{\partial R} = \left\langle \frac{\sigma_{eq} - R - \sigma_Y + h'(r)}{K} \right\rangle^N r^\gamma, \tag{48}$$

$$\dot{\boldsymbol{\varepsilon}}^i = \frac{\partial \varphi}{\partial \boldsymbol{\sigma}} = \frac{3}{2} \frac{\boldsymbol{s}}{\sigma_{eq}} \dot{r}. \tag{49}$$

Using Eq. (7), we realize that $R = h'(r)$ and then the flow law results:

$$\dot{r} = \left\langle \frac{\sigma_{eq} - \sigma_Y}{K} \right\rangle^N r^\gamma, \tag{50}$$

where we note that term $\xi(r) = r^\gamma$ acts as a term that modulates hardening.

Note also that, as opposed to previous formulations, the strain-like isotropic hardening r appears now as a parameter in the dissipation potential φ.

Applications: Grill and Sorimachi [16], reported that the best agreement between finite-element and experimental results when studying bulging in continuous casting of steel slabs, was given by means of the primary creep law obtained from constant-load isothermal tests:

$$\varepsilon = \tilde{C} \exp\left(-\frac{\tilde{Q}}{kT}\right) \sigma^n t^m. \tag{51}$$

By differentiating this expression with respect to time, and after eliminating t, it yields:

$$\dot{\varepsilon} = m\tilde{C}^{1/m} \exp\left(-\frac{\tilde{Q}}{mkT}\right) \sigma^{n/m} \varepsilon^{(m-1)/m}, \tag{52}$$

which can be identified with Eq. (48) assuming negligible elastic deformation, monotonic loading, $\sigma_Y = 0$, $\gamma = (m-1)/m$, $N = n/m$, and K expressed by Eq. (30) for $C = m\tilde{C}^{1/m}$ and $Q = \tilde{Q}/m$. Material properties were determined for a low-alloy carbon steel (0.18 wt.% C), for which Eq. (52) takes the explicit form:

$$\dot{\varepsilon} = 0.8171 \exp\left(-\frac{49\,496}{T}\right) \sigma^6 \varepsilon^{-3}. \tag{53}$$

Susuki et al. [26] proposed a strain-hardening law, identical in form to Eq. (52), to describe the behavior of the ST52 steel (0.19 wt.% C, 0.30 wt.% Si, 1.19 wt.% Mn, 0.012 wt.% P, 0.032 wt.% S, 0.11 wt.% Cr, 0.032 wt.% Mo, 0.093 wt.% Ni, 0.035 wt.% Al, 0.18 wt.% Cu, 0.0058 wt.% N, <0.004 wt.% Nb, and 0.005 wt.% V). Such relationship was established on the basis of constant-load isothermal tests, conditions that yield $\dot{\varepsilon} = \dot{\varepsilon}^i$. The explicit form of Susuki et al.'s law is

$$\dot{\varepsilon} = 2.209 \times 10^5 \exp\left(-\frac{52\,664}{T}\right) \sigma^{5.222} \varepsilon^{-0.7762}. \tag{54}$$

Susuki et al.'s and Grill and Sorimachi's primary creep curves, under particular conditions, are depicted in Fig. 7.

Kozlowski et al.'s model II [3], assuming tensile test conditions (constant strain rate) and fully developed flow, can be seen as the multiplicative law:

$$\dot{\varepsilon}^i = \tilde{C}^{1/(m+1)} \exp\left(\frac{\tilde{Q}}{(m+1)kT}\right) \sigma^{n/(m+1)} \varepsilon^{i\,m/(m+1)}. \tag{55}$$

Analogy between this equation and Eq. (48) is achieved assuming monotonic loading, $\sigma_Y = 0$, $\gamma = m/(m+1)$, $N = n/(m+1)$, and K given by Eq. (30) for $C = \tilde{C}^{1/(m+1)}$ and $Q = \tilde{Q}/(m+1)$. Table 1 lists the values of the material properties $\tilde{C}$, $\tilde{Q}/k$, n, and m. An application of this model to the thermomechanical analysis of the solidified shell of a continuously cast 304 stainless steel (0.06 wt.% C, 18 wt.% Cr, 8 wt.% Ni) inside the cooling mold is shown in the work of Moitra et al. [27]. See also Figs. 1–4.

El-Bealy [19], who had defined the material (low alloy carbon steel) behavior as steady creep from the beginning of the straightening zone in continuous casting of slabs, suggested the primary creep law

$$\dot{r} = 7.9595 \times 10^5 (T_{liq} - T)^{5.328} \sigma_{eq}^{3.199} t^{-0.5} \tag{56}$$

for the early stages. Such law, under the above considerations, takes the multiplicative form

$$\dot{r} = 6.3354 \times 10^{11} (T_{\text{liq}} - T)^{-10.656} \sigma_{\text{eq}}^{6.398} r^{-1}. \quad (57)$$

El-Bealy's primary and secondary creep laws are compared in Fig. 5.

4.3. Kinematic hardening

This hypothesis is barely mentioned in continuous casting applications. In fact, we did not find any kinematic hardening law fitting the *standard* formulation in the continuous casting bibliography.

Anand [28] avoided the kinematic hardening hypothesis by considering that in many metals structural strengthening is dominated by forest dislocations and subgrains, therefore assuming an isotropic resistance of the microstructure to inelastic flow.

Kinematic hardening should not be neglected in cyclic loading conditions because of the Bauschinger and ratchetting effects on the material. But alternating loads may only be developed when the strand is passing through the rolls, and therefore the isotropic hardening hypothesis remains acceptable to simulate the initial solidification stages in continuous casting. Furthermore, when the study involves the rolling zone, e.g. while studying unbending and bulging, authors either restricted the analysis to a segment of the strand between two rolls [16,17,19,29] or neglected the strand motion [30] (or assimilated it to discontinuous shifts [8]), thus avoiding to account for cyclic loads.

A standard viscoplastic model with combined isotropic and kinematic hardening was applied by Aliaga et al. [31] to characterize the behavior of steel during heat treatment processes, which involve temperatures lower than those we are concerned with in continuous casting applications.

On the other hand, Kozlowski et al.'s model III [3], which was modified by Huespe et al. [25] to fit the standard formulation, does not treat the Ramberg–Osgood law, Eq. (23), as the definition of a stress-like isotropic hardening variable R but as the uniaxial expression of a stress-like kinematic hardening variable $\boldsymbol{X}$ (also called the *back-stress* term). However, Kozlowski et al.'s model III cannot be extended to multiaxial states using the typical strain-like tensor variable $\boldsymbol{\alpha}$ associated to $\boldsymbol{X}$, since non-linear kinematic hardening laws like that of Eq. (44) are not allowed. An alternative consists in adding particular values of the stress and the strain to the set of internal variables to compute hardening. (Usually, those values corresponding to the stress reversal points in loading-unloading processes are used.) Such a procedure, known as modeling with updating of characteristic coefficients [1], is out of the scope of the present work.

Kozlowski et al.'s model III was widely used in steel slab continuous casting simulations, e.g. in the study of the formation of shape defects such as longitudinal off-corner depressions and near-meniscus shell distortion, the separation of the strand from the mold, cracking, and other mechanisms that can be explained from strain and stress analysis [32–36].

5. Split of rate-dependent and rate-independent deformations

Some models distinguish between the instantaneous (plastic) and creep deformations in the whole inelastic deformation process, decomposing the inelastic strain as follows:

$$\boldsymbol{\varepsilon}^{\text{i}} = \boldsymbol{\varepsilon}^{\text{p}} + \boldsymbol{\varepsilon}^{\text{c}}, \quad (58)$$

where the instantaneous strain $\boldsymbol{\varepsilon}^{\text{p}}$ is governed by plasticity theory (Section 3), while the creep strain $\boldsymbol{\varepsilon}^{\text{c}}$ obeys the viscoplasticity theory (Section 4). Therefore, the evolution of this model is controlled by

$$\dot{\boldsymbol{\varepsilon}}^{\text{i}} = \dot{\boldsymbol{\varepsilon}}^{\text{p}} + \dot{\boldsymbol{\varepsilon}}^{\text{c}} = \dot{\lambda} \frac{\partial f}{\partial \boldsymbol{\sigma}} + \frac{\partial \varphi}{\partial \boldsymbol{\sigma}}, \quad (59)$$

$$\dot{r} = -\dot{\lambda} \frac{\partial f}{\partial R} - \frac{\partial \varphi}{\partial R}, \quad (60)$$

$$\dot{\boldsymbol{\alpha}} = -\dot{\lambda} \frac{\partial f}{\partial \boldsymbol{X}} - \frac{\partial \varphi}{\partial \boldsymbol{X}}, \quad (61)$$

where the consistency parameter $\dot{\lambda}$ is determined from the consistency condition (22).

Applications: In the context of high-temperature steel modeling, the present representation has been chosen by Okamura and Kawashima [29] to study bulging in continuously cast steel slabs. The material (a low carbon steel, with 0.07 wt.% C, 0.21 wt.% Si, 0.26 wt.% Mn, 0.020 wt.% P, 0.008 wt.% S) is assumed to suffer plastic deformation instantaneously, followed by creep with the time-hardening law:

$$\dot{\varepsilon}^{\text{c}} = 3.686 \times 10^{-7} \sigma^{3.33} t^{-0.5666} \quad \text{for } t \leq 1\,\text{s}, \quad (62)$$

which it is equivalent to the strain-hardening law

$$\dot{\varepsilon}^{\text{c}} = 1.432 \times 10^{-15} \sigma^{7.683} \varepsilon^{\text{i}\,-1.307} \quad \text{for } t \leq 1\,\text{s}. \quad (63)$$

The following law was preferred for longer periods:

$$\dot{\varepsilon}^{\text{i}} = 2.943 \times 10^{-15} \sigma^{7.692} \varepsilon^{\text{i}\,-1.308} \quad \text{for } t > 1\,\text{s}. \quad (64)$$

As it can be seen, they assumed that the flow is approximately twice faster after $t = 1$ s than before $t = 1$ s.

Bohemer et al. [37] defined creep strain using either of the following laws:

$$\varepsilon^{\text{c}} = 1.418 \times 10^{7} \left[\exp\left(-\frac{7700}{T - 273} \right) \sigma_{\text{eq}} \right]^{7.134} t, \quad (65)$$

$$\varepsilon^{\text{c}} = 21.022 (1250 - T)^{-4.423} \sigma_{\text{eq}}^{4.395} t^{0.5}, \quad (66)$$

$$\varepsilon^{\text{c}} = 2365 (1227 - T)^{-5.328} \sigma_{\text{eq}}^{3.199} t^{0.5}, \quad (67)$$

which were originally proposed by Palmaers et al., Pühringer, and Bramerdorfer et al., respectively (see references in [37]). The first one derives from a Norton law

$$\dot{\varepsilon}^{\mathrm{c}} = \left[\frac{\sigma_{\mathrm{eq}}}{0.0994\exp(7700/(T-273))}\right]^{7.134}, \tag{68}$$

while the latter are equivalent to the following multiplicative laws:

$$\dot{\varepsilon}^{\mathrm{c}} = 441.92\frac{\sigma_{\mathrm{eq}}^{8.790}}{(1250-T)^{8.846}}\varepsilon^{\mathrm{c}^{-1}}, \tag{69}$$

$$\dot{\varepsilon}^{\mathrm{c}} = 5.59\times 10^{6}\frac{\sigma_{\mathrm{eq}}^{6.398}}{(1227-T)^{10.656}}\varepsilon^{\mathrm{c}^{-1}}. \tag{70}$$

Unfortunately, we were not able to reproduce any prediction of these models because of the lack of data concerning the instantaneous plastic response.

6. Unified models

Following Bodner and Partom [38], several authors assumed that elastic and inelastic strain rates are generally different from zero at all stages of loading and unloading, disregarding the existence of the yield surface postulated by the classical theories of plasticity and viscoplasticity (Sections 3 and 4). Furthermore, the irreversible deformation is accounted for in a single variable, in contrast to the development of Section 5, giving rise to the term *unified* that identifies these viscoplastic models.

Unified models usually make use of stress-like hardening variables, such as the drag-stress σ_{D} and the back-stress $\boldsymbol{X}$ for isotropic and kinematic hardening, respectively. For isotropic hardening, we can define a general flow rule as [39]

$$\dot{\boldsymbol{\varepsilon}}^{\mathrm{i}} = \frac{3}{2}\phi\left(\frac{\sigma_{\mathrm{eq}}}{\sigma_{\mathrm{D}}}\right)\frac{\boldsymbol{s}}{\sigma_{\mathrm{eq}}}. \tag{71}$$

Function ϕ has the dimensions of an inverse time and increases rapidly with this argument.

Applications: Anand [28] has formulated a unified viscoplastic model for metals at high temperatures, whose expression is

$$\dot{\varepsilon}^{\mathrm{i}} = C\exp\left(-\frac{Q}{kT}\right)\left(\frac{\sigma}{\sigma_{\mathrm{D}}}\right)^{1/m}. \tag{72}$$

The drag-stress $\sigma_{\mathrm{D}} < \sigma$ is determined by integrating the rate equation

$$\dot{\sigma}_{\mathrm{D}} = h_0\left[\dot{\varepsilon}^{\mathrm{i}} - \left(C\exp\left(-\frac{Q}{kT}\right)\right)^{n}\frac{\sigma_{\mathrm{D}}}{\tilde{\sigma}_{\mathrm{D}}}\dot{\varepsilon}^{\mathrm{i}^{1-n}}\right], \tag{73}$$

subject to the initial condition $\sigma_{\mathrm{D}} = \sigma_{\mathrm{D}_0}$, that depends on the thermal history. Material properties C, m, n, h_0, and $\tilde{\sigma}_{\mathrm{D}}$ are (eventually) thermal dependent, and were determined for a low carbon steel (0.05 wt.% C) by means of isothermal (within the austenitic range) constant strain rate (1.4×10^{-4} to $2.3\times 10^{-2}\ \mathrm{s}^{-1}$) tensile tests. Predictions from this model are compared with experimental data and results from Kozlowski et al.'s models in Fig. 8.

Anand's model was used by Ebisu et al. [40] to describe the behavior of a high carbon low-alloy steel during the entire ingot casting process.

The constitutive equation used by Lee et al. [41] and Han et al. [42] defined as:

$$\dot{r} = A\exp\left(-\frac{Q}{kT}\right)\left(\sinh\frac{\beta\sigma_{\mathrm{eq}}}{r^{n}}\right)^{1/m}, \tag{74}$$

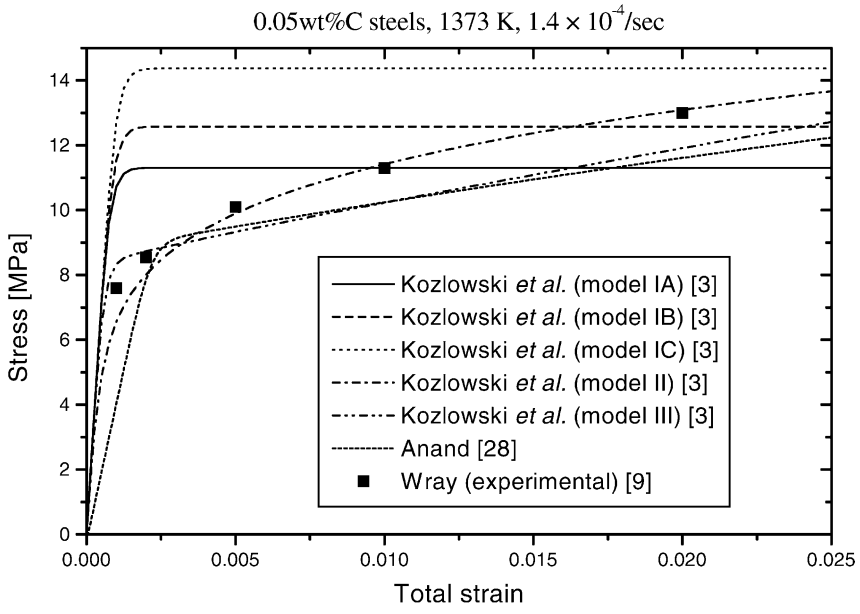

Fig. 8. Tensile curves for low carbon steels.

can also be seen as a unified viscoplastic model by identifying the drag-stress with $\beta^{-1}r^n$, and therefore its evolution is controlled by the flow rule itself.

7. Conclusions

Different material models of steel at high temperature have been analyzed and compared, placing emphasis on continuous casting processes. Laws have been put in an appropriate thermodynamic context. Several plastic and viscoplastic standard materials were considered.

This study has shown the great influence of the strain rate on the behavior of steel at elevated temperature. Therefore, considering the wide range of strain rates involved in continuous casting, rate-dependent viscoplastic models seem to be the most appropriate ones. Since hardening has been observed in all the experimental results, models allowing this phenomenon should be preferred.

However, the computational cost of viscoplastic models is usually higher than that of plastic models. Plastic models with linear isotropic hardening are particularly used in continuous casting modeling due to their easy computational implementation.

Results from different authors seem to give a wide dispersion. There is still a need for more experimental results in order to arrive to a material model that allows to predict the kind of defects that the industry is demanding (i.e. prediction of cracks formation).

References

[1] J. Lemaître, J.-L. Chaboche, Mechanics of Solid Materials, Cambridge University Press, Cambridge, 1994.
[2] P. Germain, Q.S. Nguyen, P. Suquet, Continuum thermodynamics, ASME J. Appl. Mech. 50 (4b) (1983) 1010–1020.
[3] P.F. Kozlowski, B.G. Thomas, J.A. Azzi, H. Wang, Simple constitutive equations for steel at high temperature, Metall. Trans. A 23 (1992) 903–918.
[4] B.G. Thomas, I.V. Samaresekera, J.K. Brimacombe, Mathematical model of the thermal processing of steel ingots. Part II. Stress model, Metall. Trans. B 18 (1987) 131–147.
[5] J.E. Kelly, K.P. Michalek, T.G. O'Connor, B.G. Thomas, J.A. Dantzig, Initial development of thermal and stress fields in continuosly cast steel billets, Metall. Trans. A 19 (1988) 2589–2602 (in Japanese).
[6] M.R. Ridolfi, B.G. Thomas, G. Li, U. Della Foglia, The Optimization of Mold Taper for the Ilva-Dalmine Round Bloom Caster, La Revue de Métallurgie, CIT, April 1994, pp. 609–620.
[7] J.C. Simo, T.J.R. Hughes, Computational Inelasticity, Springer, New York, 1998.
[8] M. Uehara, I.V. Samarasekera, J.K. Brimacombe, Mathematical modelling of unbending of continuously cast steel slabs, Ironmaking and Steelmaking 13 (3) (1986) 138–153.
[9] P.J. Wray, Effect of carbon content on the plastic flow of plain carbon steels at elevated temperatures, Metall. Trans. A 13 (1982) 125–134.
[10] E. Dvorkin, M. Canga, Thermomechanical behavior of the mold in siderca continuous casting machine CC3. Case of ϕ 295 mm and carbon steel 042, Technical Report I 1.20/190-90, CINI, 1990.
[11] A.E. Huespe, A. Cardona, V.D. Fachinotti, Determinación de Tensiones Térmicas en Aceros, Producidas en la Etapa Inicial del Proceso de Colada Continua, in: Mecánica Computacional AMCA, Bariloche, Argentina, vol. XVIII, 1997, pp. 185–194.
[12] A. Cardona, A. Huespe, V. Fachinotti, Modelado termo-mecánico del proceso de colada continua de aceros, in: Proceedings of the Anales del XVIII Congresso Ibero Latino-Amer. de Mét. Comp. para Eng. (XVIII CILAMCE), vol. I, Brasília, Brasil, 1997, pp. 493–500.
[13] S. Rugonyi, M. Goldschmit, E. Dvorkin, Análisis Numérico Experimental de la CC3 de SIDERCA. Informe de Avance III, Technical Report CINI I-998/96, October 1996.
[14] A.E. Huespe, A. Cardona, V. Fachinotti, Thermomechanical model of a continuous casting process, Comput. Meth. Appl. Mech. Eng. 182 (2000) 439–455.
[15] S. Sakui, T. Sakai, Deformation bevaviours of a 0.16% C steel in the austenite range, Tetsu-to-Hagané 63 (2) (1977) 285–293.
[16] A. Grill, K. Sorimachi, The thermal loads in the finite element analysis of elasto-plastic stresses, Int. J. Num. Meth. Eng. 14 (4) (1979) 499–506.
[17] J.B. Dalin, J.-L. Chenot, Finite element computation of bulging in continuously cast steel with a viscoplastic model, Int. J. Num. Meth. Eng. 25 (1988) 147–163.
[18] J.O. Kristiansson, Thermal stresses in the early stage of solidification of steel, J. Therm. Stresses 5 (1982) 315–330.
[19] M. El-Bealy, On the mechanism of halfwaycracks and macrosegregation in continuously cast steel slabs. I. Halfway cracks, Scand. J. Metall. 24 (1995) 63–80.
[20] J.R. Williams, R.W. Lewis, K. Morgan, An elasto-viscoplastic thermal stress model with applications to the continuous casting of metals, Int. J. Num. Meth. Eng. 14 (1) (1979) 1–10.
[21] R.W. Lewis, K. Morgan, P.M. Roberts, Determination of thermal stresses in solidification problems, in: J.F.T. Pittman, O.C. Zienkiewicz, R.D. Wood, J.M. Alexander (Eds.), Numerical Analysis of Forming Processes, Wiley, New York, 1984, Chapter 15, pp. 405–431.
[22] T. Inoue, Metallo-thermo-mechanical coupling. Application to the analysis of quenching, welding and continuous casting processes, Berg- und Hüttenmännische Monatshefte 132 (3) (1987) 63–71.
[23] M. Bellet, F. Decultieux, M. Ménaï, F. Bay, C. Levaillant, J.-L. Chenot, P. Schmidt, I.L. Svensson, Thermomechanics of the cooling stage in casting processes: three-dimensional finite element analysis and experimental validation, Metall. Mater. Trans. B 27 (1996) 81–99.
[24] B.Q. Li, Y. Ruan, Integrated finite element model for transient fluid flow and thermal stresses during continuous casting, J. Therm. Stresses 18 (1995) 359–381.
[25] A.E. Huespe, A. Cardona, N. Nigro, V. Fachinotti, Viscoplastic constitutive models of steel at high temperature, J. Mater. Proc. Technol. 102 (2000) 143–152.
[26] T. Susuki, K.-H. Tacke, K. Wünnemberg, K. Schwerdtfeger, Creep properties of steel at continuous casting temperatures, Ironmaking and Steelmaking 15 (2) (1988) 90–100.
[27] A. Moitra, B.G. Thomas, W. Storkman, Thermo-mechanical model of steel shell behavior in continuous casting mold, in: Proceedings of the TMS Annual Meeting, San Diego, CA, March 1992.
[28] L. Anand, Constitutive equations for the rate-dependent deformation of metals at elevated temperatures, ASME J. Eng. Mater. Technol. 104 (1982) 12–17.
[29] K. Okamura, H. Kawashima, Three-dimensional elasto-plastic and creep analysis of bulging in continuously cast slabs, ISIJ Int. 29 (1989) 666–672.
[30] K. Harste, M. Deisinger, I. Steinert, K.-H. Tacke, Thermische und mechanische MODELLE zur Stranggießen, Stahl und Eisen 115 (4) (1995) 111–118.
[31] C. Aliaga, E. Massoni, J.L. Treuil, 3D Numerical simulation of THEVP behavior using stabilized mixed F.E. formulation: application to 3D heat treatment, in: S. Idelsohn, E. Oñate, E. Dvorkin

(Eds.), Computational Mechanics: New Trends and Applications, CIMNE, Barcelona, Spain, 1998.

[32] A. Moitra, B.G. Thomas, H. Zhu, Application of a thermo-mechanical model for steel behavior in continuous slab casting, in: Proceedings of the 76th Steelmaking Conference, Dallas, TX, March 1993, pp. 657–667.

[33] B.G. Thomas, A. Moitra, H. Zhu, Coupled thermo-mechanical model of solidifying steel shell applied to depression defects in continuous-cast slabs, in: Proceedings of the Modeling of Casting, Welding, and Advanced Solidification Processes VII, London, September 1995.

[34] B.G. Thomas, H. Zhu, Thermal distortion of solidifying shell near meniscus in continuous casting of steel, in: Proceedings of the JIM/JTS Solidification Science and Processing Conference, Honolulu, HI, December 1995.

[35] B.G. Thomas, A. Moitra, R. McDavid, Simulation of longitudinal off-corner depressions in continuously cast steel slabs, in: Proceedings of the Iron & Steel Society's Process Technology Conference, vol. 13, Nashville, TN, 1996, pp. 143–156.

[36] B.G. Thomas, J.T. Parkman, Simulation of thermal mechanical behaviour during initial solidification, in: Proceedings of the Thermec'97 International Conference on Thermomechanical Processing of Steel and Other Materials, Wollongong, Australia, July 1997.

[37] J.R. Bohemer, F.N. Fett, G. Funk, Analysis of high-temperature behaviour of solidified material within a continuous casting machine, Comp. Struct. 47 (4/5) (1993) 683–698.

[38] S.R. Bodner, Y. Partom, A large deformation elastic-viscoplastic analysis of a thick-walled spherical shell, ASME J. Appl. Mech. 39 (1972) 751–757.

[39] J. Lubliner, Plasticity Theory, Macmillan, New York, 1990.

[40] Y. Ebisu, K. Sekine, M. Hayama, Analysis of thermal and residual stresses of a low alloy cast steel ingot by the use of viscoplastic constitutive equations considering phase transformations, Tetsuo-to-Hagané 78 (6) (1992) 894–901 (in Japanese).

[41] J.-E. Lee, H.N. Han, K.H. Oh, J.-K. Yoon, A fully coupled analysis of fluid flow, heat transfer and stress in continuous round billet casting, ISIJ Int. 39 (5) (1999) 435–444.

[42] H.N. Han, J.-E. Lee, T.-J. Yeo, Y.M. Won, K.-H. Kim, K.H. Oh, J.-K. Yoon, A finite element model for 2-dimensional slice of cast strand, ISIJ Int. 39 (5) (1999) 445–454.